Neuron, Vol. 20, 55–67, January, 1998, Copyright ©1998 by Cell Press

The Gα Protein ODR-3 Mediates Olfactory and Nociceptive Function and Controls Cilium Morphogenesis in *C. elegans* Olfactory Neurons

Kayvan Roayaie,* Justin Gage Crump,* Alvaro Sagasti, and Cornelia I. Bargmann†
Howard Hughes Medical Institute
Programs in Developmental Biology, Neuroscience, and Genetics
Department of Anatomy
University of California
San Francisco, California 94143

Summary

The G_i/G_o-like Gα protein ODR-3 is strongly and selectively implicated in the function of *C. elegans* olfactory and nociceptive neurons. Either loss of *odr-3* function or overexpression of *odr-3* causes severe olfactory defects, and *odr-3* function is essential in the ASH neurons that sense noxious chemical and mechanical stimuli. In the nociceptive neurons, ODR-3 may interact with OSM-9, a channel similar to the mammalian capsaicin receptor implicated in pain sensation; in AWC olfactory neurons, ODR-3 may interact with another signal transduction pathway. ODR-3 exhibits an unexpected ability to regulate morphogenesis of the olfactory cilia. In *odr-3* null mutants, the fan-like AWC cilia take on a filamentous morphology like normal AWA cilia, whereas ODR-3 overexpression in AWA transforms its filamentous cilia into a fan-like morphology.

Introduction

Many sensory neurons have elaborate cilia that contribute to sensory function through their structural properties and their localization of signaling proteins (Barber, 1974; Tamar, 1992). Specialized vertebrate sensory cilia include the outer segments of rod and cone photoreceptors, the kinocilium associated with the stereocilia of vertebrate mechanosensory and auditory hair cells, and olfactory cilia (Figure 1A). Little is known about the mechanisms by which these specialized cilia are generated and shaped.

Olfactory cilia are the site at which odorants first interact with olfactory receptor proteins. In the nematode *C. elegans*, olfaction is mediated by ciliated neurons that are associated with the two amphid chemosensory organs (Bargmann and Mori, 1997). *C. elegans* senses volatile attractants using two pairs of olfactory neurons: the AWA neurons mediate responses to diacetyl and pyrazine, and the AWC neurons mediate responses to benzaldehyde, isoamyl alcohol, and 2-butanone (Bargmann et al., 1993). Like olfactory neurons in other animals, these neurons have elaborate cilia (Figures 1B and 1C; Ward et al., 1975; Ware et al., 1975). The AWA cilia are filamentous and extensively branched, whereas the AWC cilia form a large sheet of membrane that encircles the tip of the nose (Ward et al., 1975; Ware et al., 1975; Perkins et al., 1986). Water-soluble attractants, repellents, and pheromones are sensed by amphid-associated neurons with simple single or double cilia (e.g., ASE and ASH neurons).

C. elegans detects odors using receptors such as the diacetyl receptor ODR-10, a predicted G protein–coupled receptor that is localized to the AWA olfactory cilia (Sengupta et al., 1996). *odr-10* mutants have a specific defect in their ability to detect the odorant diacetyl, and heterologous expression of ODR-10 in ectopic *C. elegans* neurons or human 293 cells confers diacetyl responsiveness on those cells (Troemel et al., 1997; Zhang et al., 1997). ODR-10 is unrelated in sequence to the mammalian olfactory or vomeronasal receptors, but it has seven transmembrane domains and key residues characteristic of G protein–coupled receptors. About 200 additional *odr-10*–like genes and an equal number of genes from other potential families of G protein–coupled receptors might encode other chemosensory receptors in *C. elegans* (Troemel et al., 1995; E. Troemel and C. I. B., unpublished data).

Two types of *C. elegans* sensory channels have been identified by analyzing mutants with olfactory defects. AWC-mediated olfaction requires the activity of a cyclic nucleotide–gated channel encoded by the *tax-2* and *tax-4* genes (Coburn and Bargmann, 1996; Komatsu et al., 1996). The TAX-2/TAX-4 channel is similar to the vertebrate visual and olfactory channels and implicates cGMP or cAMP as a second messenger in *C. elegans* sensory pathways. It is also required in sensory neurons that detect water-soluble attractants (ASE) and thermal gradients (AFD). AWA-mediated olfaction is generated by an alternative pathway that requires a novel putative channel encoded by the *osm-9* gene (Colbert et al., 1997). *osm-9* is also required for avoidance of noxious osmotic, volatile, and mechanical stimuli that are detected by the ASH sensory neurons. The dual mechanical and chemical sensitivity of ASH is reminiscent of pain-sensing (nociceptive) neurons in vertebrates (Kaplan and Horvitz, 1993). Amazingly, OSM-9 has extensive similarity to the capsaicin receptor, which is implicated in vertebrate pain sensation (Caterina et al., 1997; Colbert et al., 1997). Both of these channels are distantly related to the *Drosophila* phototransduction channel TRP, which is regulated by G protein signaling (Tsunoda et al., 1997).

Many G proteins are implicated in vertebrate and invertebrate olfaction. In the vertebrate olfactory system, odorants increase levels of cAMP, which opens an olfactory cyclic nucleotide–gated channel in the olfactory cilia (Pace et al., 1985; Firestein et al., 1991). The G_s-like G_{olf} protein is concentrated in the ciliated sensory endings of the olfactory neurons, suggesting that it mediates the odor-induced increases in cAMP (Jones and Reed, 1989). Indeed, G_{olf} mutant mice have profound defects in odorant-induced activity (Belluscio et al., 1998 [this issue of *Neuron*]). Mammalian vomeronasal neurons,

*These authors contributed equally to this work.
†To whom correspondence should be addressed.

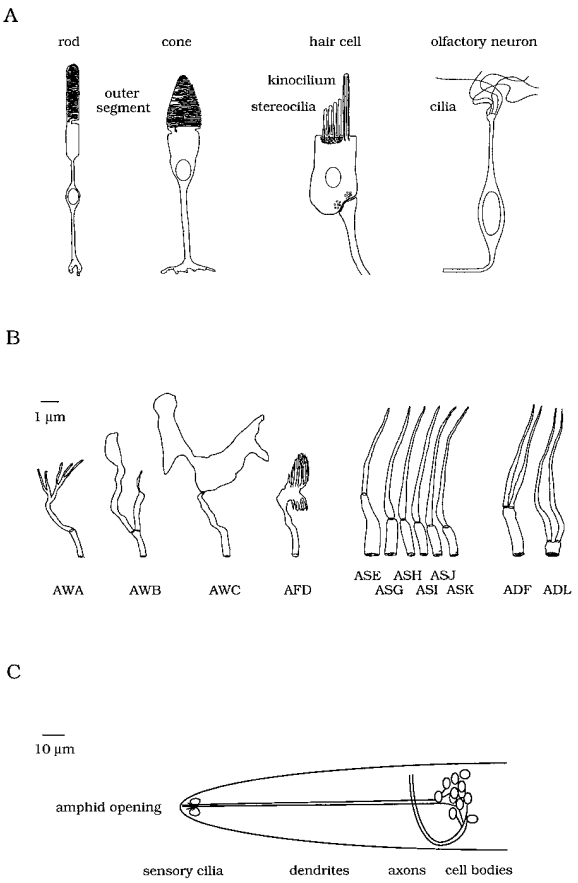

Figure 1. Morphologies of Sensory Cilia

(A) Cilium morphologies of vertebrate photoreceptors (rods and cones), mechanoreceptors (hair cells), and olfactory neurons. The entire cell is shown in each case (except for the olfactory axon); drawings are not to scale.

(B) *C. elegans* cilium morphologies, adapted from Perkins et al. (1986). The ciliated endings of these sensory neurons are associated with the amphid opening at the tip of the nose. All have one or two transition zones at the base of the cilia (in the AFD neurons, this zone is embedded within one of the projections). The actual AWA morphology is probably much more complex than was appreciated from these electron micrograph reconstructions (see Figure 6).

(C) Overall structure of the amphid sensory organ. The bilaterally symmetric amphids each contain the endings of 11 chemosensory neurons and one thermosensory neuron. Only the left side is shown. At the tip of the nose, a small opening exposes the cilia of the ASE, ASG, ASH, ASI, ASJ, ASK, ADF, and ADL neurons. The AWA, AWB, and AWC cilia are enclosed within a sheath pocket that is continuous with the environment, and the thermosensory AFD neurons are not exposed. Anterior is at left and dorsal is up.

which detect pheromones, express either G_{i2} or G_o but not G_{olf} (Halpern et al., 1995; Berghard and Buck, 1996). The targets of G_{i2} and G_o in the vomeronasal system are unknown. Another signaling pathway is used in insect olfaction, which expresses a specialized G_q protein and requires phospholipase C activity for olfactory transduction (Woodard et al., 1992; Talluri et al., 1995). Sensation of sweet and bitter taste in vertebrates requires a transducin-like Gα protein, gustducin, which might regulate phosphodiesterases in taste cells (Ruiz-Avila et al., 1995; Wong et al., 1996).

C. elegans odr-3 mutants were isolated in a behavioral screen for animals that failed to chemotax to benzaldehyde (Bargmann et al., 1993). They have diminished responses to all odorants detected by the AWA and AWC neurons, but they retain responses to high concentrations of odorants. They are also defective in the chemosensory and mechanosensory functions of the ASH neurons. Here, we show that *odr-3* encodes a G_i-like Gα protein that is expressed in AWA, AWC, ASH, and two other pairs of chemosensory neurons. Although it is coexpressed in sensory neurons with similar *gpa* Gα proteins, *odr-3* and the *gpa* genes have mostly distinct functions. The ODR-3 protein is localized to the sensory cilia, where the initial events of odorant detection occur. *odr-3* activity affects morphogenesis of the AWA and AWC cilia, suggesting that this Gα protein specifies one aspect of cilium morphology.

Results

odr-3 Encodes a G Protein α Subunit

odr-3 was cloned by rescue of its osmotic avoidance phenotype with cosmid clones and subclones from the genetically defined *odr-3* interval (Figure 2A and Experimental Procedures). The coding sequence of a novel Gα subunit was entirely contained on pODR3-1, a clone that rescued *odr-3* mutants. Three subclones that failed to rescue *odr-3* disrupted the Gα gene, identifying it as the likely *odr-3* coding region.

A full-length *odr-3* cDNA was isolated and sequenced (see Experimental Procedures). *odr-3* encodes a predicted protein of 356 amino acids that is a member of the Gα family and shares the highest degree of homology (57% amino acid identity) with *gpa-3* (G protein α; Lochrie et al., 1991), a sensory Gα protein from *C. elegans* (Figures 2B, 2C, and 2D). With respect to the vertebrate classes of Gα subunits, *odr-3* is most closely related to the G_i/G_o family (47% amino acid identity to G_{i2}). This similarity is less striking than the similarity between *C. elegans* homologs of G_o, G_q, and G_s and their vertebrate counterparts, which share >68% amino acid identity (Mendel et al., 1995; Segalat et al., 1995; Brundage et al., 1996; Korswagen et al., 1997).

The amino terminus of ODR-3 contains consensus sites for myristylation and palmitoylation (daggers in Figure 2B), posttranslational modifications that can localize Gα proteins to the plasma membrane (Wedegaertner et al., 1995). The Gα residues important in guanine nucleotide binding and GTP hydrolysis are conserved in ODR-3 (boldface in Figure 2B; Rens-Domiano and Hamm, 1995). The carboxyl termini of Gα subunits are important in defining their interactions with seven transmembrane-domain receptors (Conklin and Bourne, 1993); this region of ODR-3 is unique.

odr-3 Null Mutants Are Defective in Olfaction and in Olfactory, Osmotic, and Mechanosensory Avoidance

An independent mutant screen for osmotic avoidance–defective mutants led to the isolation of an additional allele of *odr-3, n1605* (J. H. Thomas, personal communication). To determine whether all *odr-3* phenotypes were

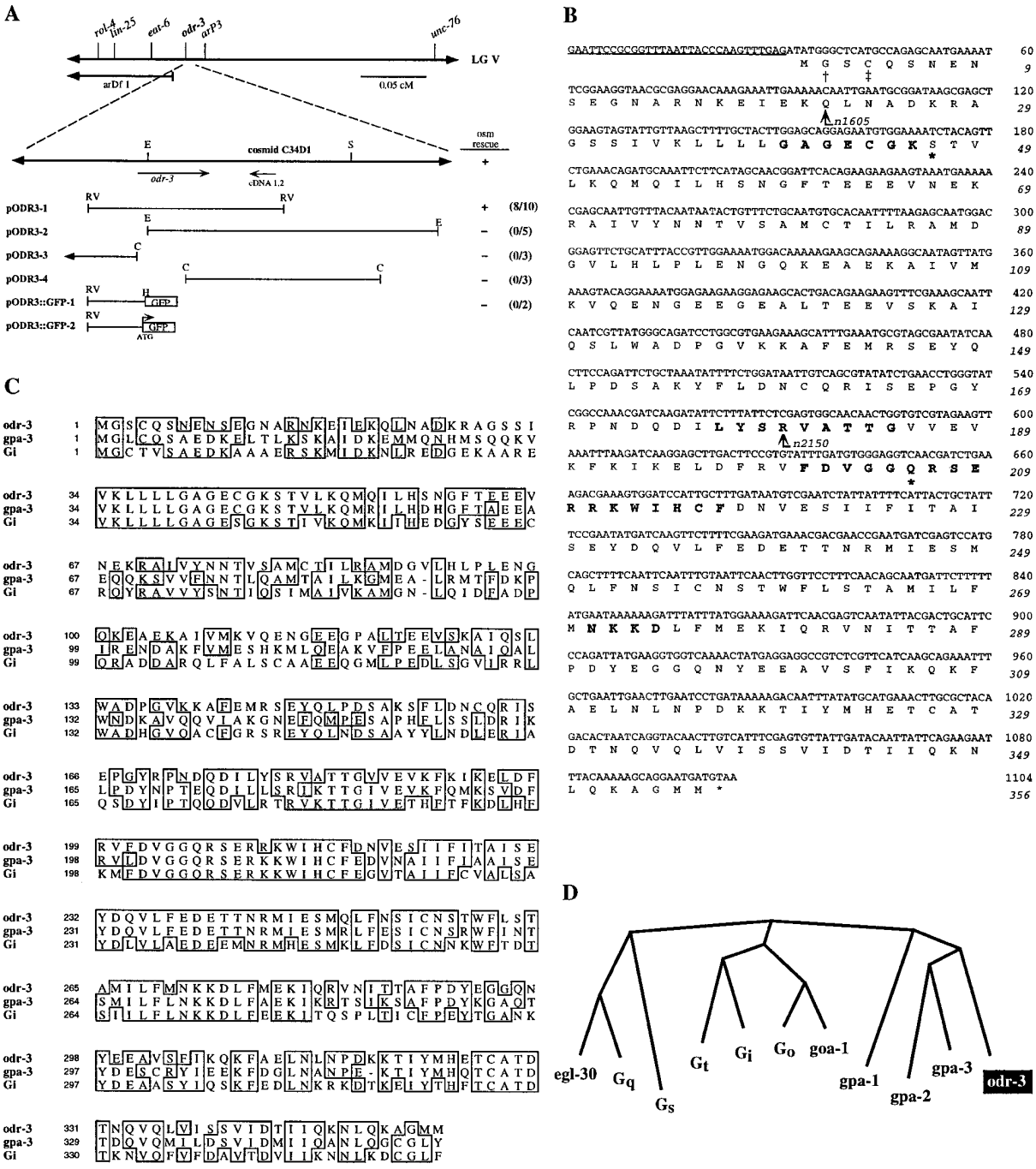

Figure 2. *odr-3* Encodes a G Protein α Subunit

(A) Genetic and physical maps of the *odr-3* region. Genetic map data were used to localize *odr-3* between *eat-6* and *arP3*. One cosmid within that region, C34D1, contains *odr-3* rescuing activity, as does pODR3-1. pODR3-2, pODR3-3, and pODR3-4 did not rescue *odr-3* mutants. Clones were tested for rescue of the Osm phenotype of *odr-3*; the number of independent lines with rescue of this phenotype is shown as a ratio of the total number of independent lines that were tested. pODR3::GFP-1 includes the first 36 amino acids of *odr-3*, whereas pODR3::GFP-2 fuses GFP precisely to the initiator methionine of *odr-3*.

(B) DNA and protein sequence of *odr-3*. A full-length *odr-3* cDNA was sequenced in its entirety. The SL1 splice leader sequence at the 5′ end of the gene is underlined. Conserved Gα regions involved in GTP binding are in boldface type. Residues that are changed to stop codons in *odr-3* mutants are marked with arrows, whereas residues that were mutagenized in this work are marked with asterisks. Potential sites of posttranslational modification are marked with a dagger (myristylation) or a double dagger (palmitoylation).

(C) Alignment of *odr-3* with the *C. elegans gpa-3* gene and rat $G\alpha_{i2}$, generated using Clustal W (Thompson et al., 1994). Identical residues are boxed.

(D) A parsimonious tree of vertebrate G proteins, *C. elegans* G_o (goa-1) and G_q (egl-30) proteins, and the *C. elegans* gpa and odr-3 proteins, generated using the Phylip program (Felsenstein, 1996).

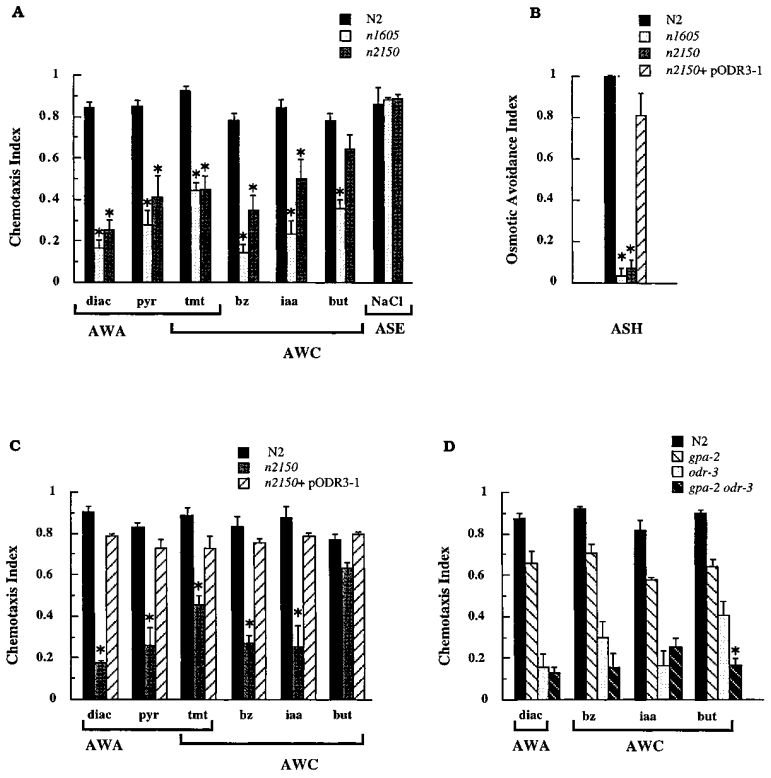

Figure 3. Behavioral Phenotypes of *odr-3* Mutants and Rescued Strains

(A) Chemotaxis responses of wild-type, *odr-3(n1605)*, and *odr-3(n2150)* strains. For all figures, abbreviations are as follows: diac, 1:1000 dilution of diacetyl; pyr, 10 mg/ml pyrazine; tmt, 1:1000 2,4,5-trimethylthiazole; bz, 1:200 benzaldehyde; iaa, 1:100 isoamyl alcohol; but, 1:1000 2-butanone; and NaCl, 0.2 M NaCl. All volatile odorants were diluted in ethanol. Asterisks denote numbers different from the control at $p < 0.01$. *odr-3(n1605)* was different from *odr-3(n2150)* for chemotaxis to 2-butanone ($p = 0.001$) and marginally different for chemotaxis to benzaldehyde ($p = 0.023$) and isoamyl alcohol ($p = 0.03$). There could be a residual function of the truncated *odr-3* protein in *odr-3(n2150)*, or these differences could be caused by other strain differences.

(B) Osmotic-avoidance responses of wild-type animals, *odr-3* mutants, and *odr-3(n2150)* mutants rescued with pODR3-1 DNA (10 ng/μl injection).

(C) Chemotaxis responses of wild-type animals, *odr-3(n2150)* mutants, and *odr-3(n2150)* mutants rescued with pODR3-1 DNA (10 ng/μl injection).

(D) Mutant phenotypes of *odr-3(n1605)*, *gpa-2(pk16)*, and *gpa-2(pk16) odr-3(n1605)* mutants. The *gpa-2 odr-3* double mutants differ from each single mutant at $p < 0.01$ (asterisk) for butanone chemotaxis; for all other odorants, double mutants were no more severe than *odr-3* alone.

Chemosensory neurons responsible for directing each response are listed under the odorant or assay. For all assays, controls were tested in parallel on the same day as the mutant strains to control for day-to-day variation of the assay. At least three independent assays were conducted for each data point. Error bars indicate the standard error of the mean (SEM).

caused by the same gene, we compared the behavioral effects of the independent *odr-3(n2150)* and *odr-3(n1605)* mutations. Like *odr-3(n2150)* animals, *odr-3(n1605)* mutants were defective in chemotaxis to all volatile attractants, including odorants sensed by both the AWA and the AWC olfactory neurons (Figure 3A). The severity of the mutant defects varied from mild (e.g., butanone chemotaxis) to severe (e.g., diacetyl chemotaxis). In all cases, *odr-3(n1605)* was comparable or more defective in its responses than *odr-3(n2150)*. Both alleles displayed normal chemotaxis to water-soluble attractants such as NaCl (Figure 3; data not shown). All of the olfactory defects of *odr-3(n2150)* mutants were rescued by the *odr-3* transgene, confirming that they were all caused by the same mutation (Figure 3C).

odr-3 mutants were defective in all avoidance responses mediated by the ASH sensory neurons. The ASH neurons are essential for osmotic avoidance and avoidance of light touch to the nose, both of which were defective in the *odr-3(n1605)* and *odr-3(n2150)* mutants (Figure 3B; data not shown). *odr-3* mutants were also highly defective in avoidance of the volatile repellent octanol in an assay that depends on ASH and ADL (data not shown).

The coding region of *odr-3* was sequenced in *n1605* and *n2150* mutants to determine the nature of the *odr-3* mutations (Figure 2B). Each mutant allele had a G-to-A transition mutation, consistent with the mutagenic spectrum of the mutagen ethylmethanesulfate. In *odr-3(n1605)* animals, a glutamine at amino acid residue 22 was changed to a stop codon. This early nonsense mutation in the coding sequence suggests that *n1605* results in a complete loss of *odr-3* function. In *odr-3(n2150)* animals, an arginine at amino acid residue 180 was changed to a stop codon. This nonsense mutation would only produce the amino-terminal half of the protein, which would not function properly as a Gα but might retain some ability to bind Gβγ subunits (Conklin and Bourne, 1993). The weaker behavioral phenotype of *odr-3(n2150)* may be due to activity of this partial protein, or it may be due to other differences in the strain backgrounds.

These behavioral data indicate that *odr-3* is essential for all AWA and ASH functions but less critical for some AWC responses. The mild butanone defects of *odr-3* null mutants suggest that a different Gα protein may mediate responses to some odorants. The Gα protein GPA-2 is expressed in the AWC neurons that detect butanone (Zwaal et al., 1997). *gpa-2* null mutants had nearly normal olfactory responses, including strong butanone chemotaxis (Figure 3D). However, *gpa-2 odr-3* double mutants were highly defective in butanone chemotaxis, indicating that the two G proteins act redundantly in the response to this odorant (Figure 3D).

odr-3 Is Expressed in a Subset of Sensory Neurons

In order to identify the cells that express *odr-3*, ~2.7 kb of the *odr-3* promoter was used to drive expression of

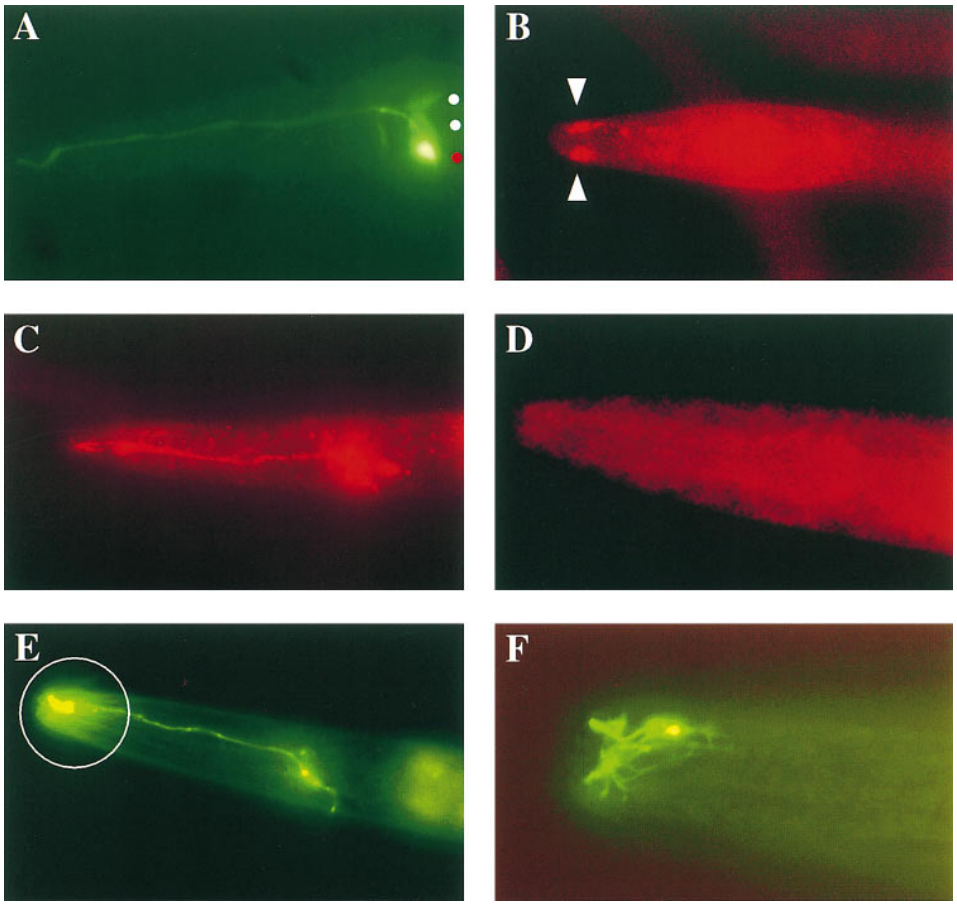

Figure 4. Expression of Endogenous ODR-3 Protein and *odr-3* Fusion Genes

(A) Expression of pODR3::GFP-2, a transcriptional fusion of GFP to the initation codon of *odr-3* (Figure 2A; lateral view). Strong expression in the AWC neuron is visible (red dot), along with weaker expression in ASH and AWB (white dots).

(B) Expression of endogenous ODR-3 protein in the cilia of the AWC neurons (arrowheads), detected with anti-ODR3 antisera (dorsal view).

(C) Expression of ODR-3 protein overexpressed from its own promoter (the plasmid pODR3-1, injected at 100 ng/μl), detected with anti-ODR3 antisera (lateral view). A cluster of cell bodies is visible, along with their sensory processes.

(D) ODR-3 expression is not detectable with anti-ODR3 antisera in the *odr-3(n1605)* mutant strain.

(E) Expression of pODR3::GFP-1, a translational fusion that incorporates the first 36 amino acids of ODR-3 into the fusion protein (lateral view). Expression is highly concentrated in the cilia (circled).

(F) High magnification view of the AWC cilia expressing pODR3::GFP-1.

the green fluorescent protein (GFP) in transgenic animals (Chalfie et al., 1994). Expression of the GFP reporter gene was observed in five pairs of sensory neurons, the AWA, AWB, AWC, ASH, and ADF neurons (Figure 4A). The AWC neurons consistently expressed GFP most brightly, the AWB neurons less well, and the AWA, ASH, and ADF neurons only weakly (see Experimental Procedures). The expression of *odr-3* in the AWA and AWC neurons is consistent with the observed volatile attraction defect of mutant *odr-3* mutant animals, whereas expression in ASH could account for the osmotic-avoidance, octanol-avoidance, and nose-touch defects. *odr-3* mutants are also defective in AWB-mediated long-range avoidance (Troemel et al., 1997). This restricted pattern of GFP expression suggests that *odr-3* subserves a specialized function in sensory neurons.

Antibodies against the ODR-3 protein were generated and used to detect the endogenous ODR-3 protein in wild-type and mutant animals. The anti–ODR-3 antibodies stained only the ciliated endings of a few amphid neurons in wild-type animals (Figure 4B). The AWC neurons were identified by the distinctive morphology of their ciliated endings, but the identity of the other cells expressing *odr-3* could not be established based on cilia morphology. However, the overall pattern of staining is consistent with the predicted pattern based on the GFP fusion gene, and no staining was observed outside the amphid region. To help identify the cells that expressed ODR-3, the anti–ODR-3 antibodies were also used to stain animals with high copy overexpression of the *odr-3* genomic clone. In these animals, the ODR-3 protein was detected in cell bodies as well as cilia, in a cluster of cells that appeared to be the AWA, AWB, AWC, ADF, and ASH cells that expressed *odr-3::GFP* transgenes (Figure 4C). The specificity of the antibody was confirmed by the absence of staining in the null mutant *odr-3(n1605)*, which should not express ODR-3 protein (Figure 4D).

In an effort to determine molecular cues necessary for localization of ODR-3 to the sensory cilia, portions

of ODR-3 were fused to GFP. The amino terminus of ODR-3 contains consensus sites for both myristylation and palmitoylation, posttranslational modifications that are required for proper localization and function of Gα subunits (Wedegaertner et al., 1995). When the promoter and the first 36 amino acids of the *odr-3* coding region were fused to GFP, the strongest GFP expression was observed at the tip of the nose (Figure 4E), particularly in the distinctive AWC cilia (Figure 4F). The enriched expression of this transgene in the cilia indicates that the first 36 amino acids of ODR-3 have a preference for the ciliated endings of sensory neurons.

Overexpression of ODR-3 Causes Olfactory Defects but Not Osmotic Avoidance Defects

Overexpression of a G protein that is closely involved in olfactory function might lead to defective olfactory signaling. To achieve *odr-3* overexpression, the wild-type *odr-3* rescuing genomic clone was injected into *odr-3(+)* animals at 10-fold higher concentrations than were typically used to rescue the mutant phenotype. All five resulting overexpressing strains *(odr-3[xs]* strains) were found to have olfactory defects. One line carrying an extrachromosomal transgenic array was characterized in more detail. As was anticipated, this line had a much higher level of ODR-3 protein expression than wild-type animals (Figure 4C), and expression appeared to be restricted to the correct sensory neurons, albeit delocalized within those cells.

Overexpression of ODR-3 resulted in olfactory defects that were as strong or stronger than those of *odr-3(n1605)* animals (Figure 5A). The *odr-3(xs)* animals were severely defective in responses to all odorants sensed by both the AWA and AWC neurons, including odorants such as 2-butanone that were only mildly affected in the null mutants. However, animals overexpressing ODR-3 were not significantly defective in osmotic avoidance (Figure 5B). The absence of an osmotic-avoidance defect is unlikely to be due to low levels of ODR-3 in the ASH neurons, since anti–ODR-3 antibodies appeared to show similar staining of ASH, AWA, and AWC neurons in the *odr-3(xs)* strain (Figure 4C).

A clone in which the *odr-3* promoter was used to drive GFP did not cause olfactory defects when injected into *odr-3(+)* animals at high concentrations (data not shown). Therefore, high levels of the *odr-3* promoter did not disrupt expression of *odr-3* or other genes involved in olfactory behaviors. Nomarski microscopy and antibody staining of *odr-3(xs)* animals revealed that the olfactory neurons were not killed by the transgene. Thus, both the absence of *odr-3* function and excessive ODR-3 protein can disrupt olfactory responses.

Constitutively Active *odr-3* Causes Olfactory and Osmotic Avoidance Defects

The overexpression of ODR-3 could disrupt olfaction either through excessive Gα activity or through titration of free $G_{\beta\gamma}$ subunits by high levels of ODR-3 protein. In all known Gα proteins, an even higher level of Gα activity can be provided by generating constitutively active alleles. Altering the conserved glutamine corresponding to ODR-3 residue 206 to leucine leads to constitutive Gα activity by blocking the GTPase activity of Gα proteins including G_s, G_q, G_o, and G_i (Conklin and Bourne, 1993; Rens-Domiano and Hamm, 1995). By analogy with these well-characterized proteins, an activated ODR-3 protein (ODR-3*) should have more Gα activity than a comparable wild-type ODR-3 protein, but it should have less ability to titrate $G_{\beta\gamma}$ subunits.

Expression of ODR-3* at high levels *(odr-3*[Q206L]xs)* caused olfactory defects in a wild-type background (Figure 5C) and also caused defects in osmotic avoidance that were not seen with expression of the wild-type ODR-3 protein (Figure 5D). The osmotic-avoidance defects caused by this mutant but not by the wild-type protein implicate Gα in ASH signaling. Only slight defects were observed when this mutant was expressed at low levels.

Expression of either *odr-3*(Q206L)* or a second point mutant *odr-3(S47C)* at low levels did not rescue the olfactory or osmotic-avoidance defects of an *odr-3* mutant (Figures 5C–5F). *odr-3(S47C)* has a serine-to-cysteine mutation at residue 47; in G_o or G_i, a similar mutation produces a G protein that retains the ability to bind $G_{\beta\gamma}$ subunits but has reduced affinity for GTP (Slepak et al., 1993, 1995). Thus, either ODR-3*(Q206L) or ODR-3(S47C) proteins might possess some Gα activity, but neither should be modulated normally by receptors. Since these point mutations eliminate the normal rescuing activity of *odr-3,* it is likely that regulated *odr-3* activity, rather than some absolute level of ODR-3 protein, is essential for normal chemosensation. The *odr-3(S47C)* clone caused a moderate olfactory defect when expressed at high levels in a wild-type background, but it did not affect osmotic avoidance (Figures 5E and 5F).

odr-3 Activity Specifies the Fan-like Morphology of the AWC Cilia

The AWC neurons have cilia that form two extended, fan-like membrane sheets, while the AWA neurons have multiply branched filamentous cilia that are condensed around microtubules (Figure 1B; Ward et al., 1975; Ware et al., 1975; Perkins et al., 1986). In previous electron micrographs of *odr-3(n2150)* mutants, we noted that the AWC cilia were reduced in size (Bargmann et al., 1993). These ultrastructural defects suggest that mutations in *odr-3* affect AWC morphology. To examine the structure of the AWA and AWC neurons in greater detail, we made use of GFP fusion proteins that reveal individual olfactory cilia. An ODR-10::GFP fusion protein is localized to the AWA cilia (Sengupta et al., 1996), whereas an STR-2::GFP fusion protein is expressed at high levels in the AWC cilia (E. Troemel, personal communication; Figures 6A and 6F). *odr-10::GFP* or *str-2::GFP* transgenes were crossed into *odr-3(n1605)*, *odr-3(xs)*, *odr-3*(Q206L)xs*, and *odr-3(S47C)xs* strains. In all of these mutants, ODR-10::GFP was expressed in AWA and STR-2::GFP was expressed in AWC, indicating that the AWA and AWC cell fates were determined correctly.

As expected from the electron micrographs, *odr-3* loss-of-function mutations led to alterations in the AWC cilia (Figure 6B). These defects were examined using conventional and wide-field deconvolution microscopy (Hiraoka et al., 1991). In *odr-3(n1605)* mutants, AWC cilia

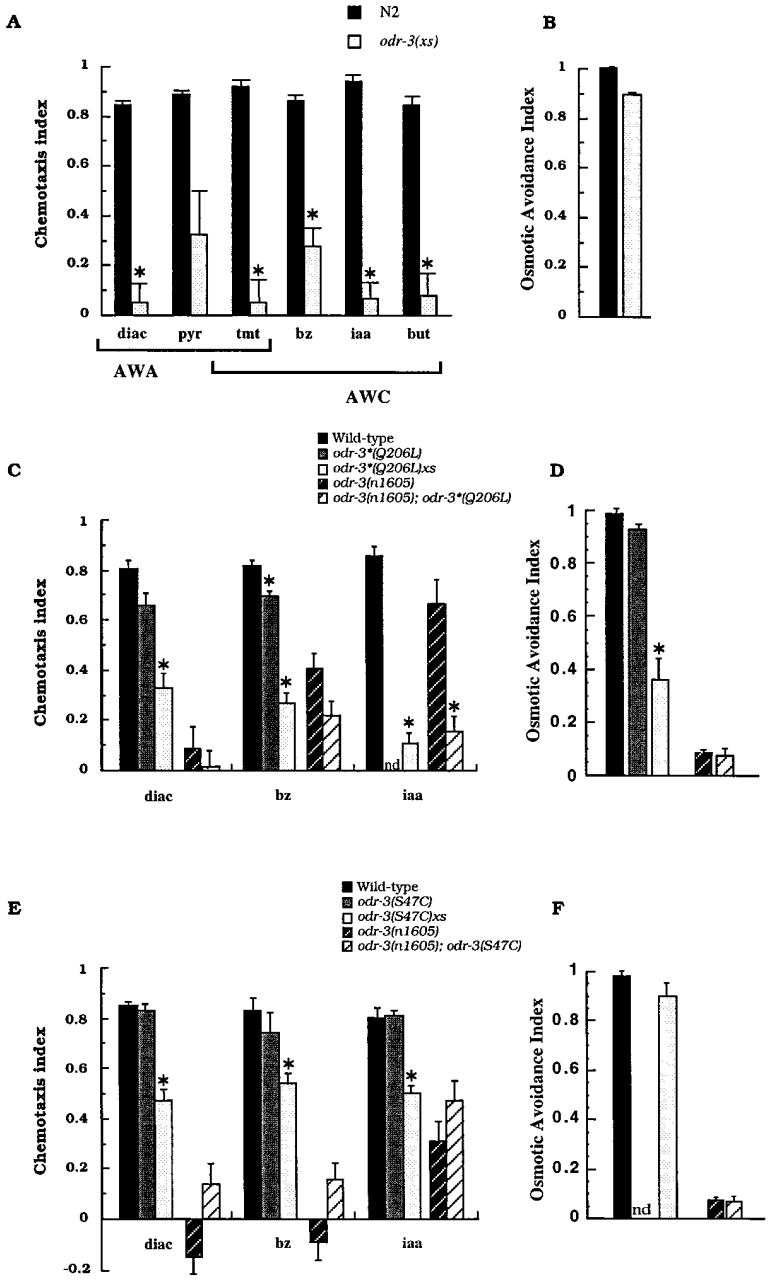

Figure 5. Behavioral Phenotypes of *odr-3* Overexpression and of *odr-3* Point Mutants

Chemotaxis responses ([A], [C], and [E]) and osmotic avoidance responses ([B], [D], and [F]) of wild-type animals (closed bars), wild-type animals bearing *odr-3* clones injected at 10 ng/μl (medium grey bars), and wild-type animals bearing *odr-3* clones injected at 100 ng/μl (open bars). *odr-3* mutant animals (closed cross-hatched bars) and *odr-3* mutants with clones injected at 10 ng/μl (open cross-hatched bars) are also included (compare injection of wild-type *odr-3* clones in Figures 3B and 3C). Asterisks denote values that are different from the controls at $p < 0.01$. Clones injected into *odr-3(+)* strains were compared to wild-type controls; clones injected into *odr-3(n1605)* were compared to *odr-3(n1605)* controls. When the wild-type clone was injected into *odr-3* mutants at 100 ng/μl, it rescued osmotic avoidance to wild-type levels, but it did not rescue diacetyl or benzaldehyde chemotaxis, presumably because it was overexpressed (data not shown). Each data point represents at least three independent assays. For the mutated *odr-3* clones, at least three independent transgenic lines were generated for each genotype and DNA concentration, and all behaved comparably in all assays. Error bars indicate the SEM.

always had filamentous branches, like AWA, instead of the extended fan-like sheets typical for AWC (n = 112 animals). The filamentous branches were often very long, perhaps to accommodate the excess AWC membrane. The AWA cilia were apparently normal in *odr-3(n1605)* mutants (n = 38).

Surprisingly, overexpression of *odr-3* led to reciprocal effects on the morphology of the AWA cilia (Figure 6G). In the *odr-3(xs)* strain, some branches of the AWA cilia were not filamentous but rather flattened and extended like AWC cilia, whereas most AWC cilia maintained the normal fan-like cilium morphology (Figures 6C and 6G; 62% of AWA cilia [n = 50] but only 13% of AWC cilia [n = 105] had altered morphologies). Thus, in either AWA or AWC, a low level of ODR-3 protein correlated with AWA-like filamentous cilia, whereas a high level specified AWC-like fan-like cilia. This morphological effect was superimposed on a normal branching pattern; in all mutants, the AWA cilia split into many branches, whereas the AWC cilia had only one or two branches.

Although overexpression of wild-type *odr-3* did not disrupt AWC morphogenesis, both the *odr-3*(Q206L)xs* strain and the *odr-3(S47C)xs* strain had highly aberrant, short filamentous AWC cilia (Figures 6D and 6E). Due to variable expression of the transgene, it was not possible to score the AWA cilia in *odr-3*(Q206L)xs* or *odr-3(S47C)xs* strains.

The ASH neurons display a normal morphology in electron micrographs from *odr-3(n2150)* animals (Bargmann et al., 1993). Disruption of the ASH cilia can be

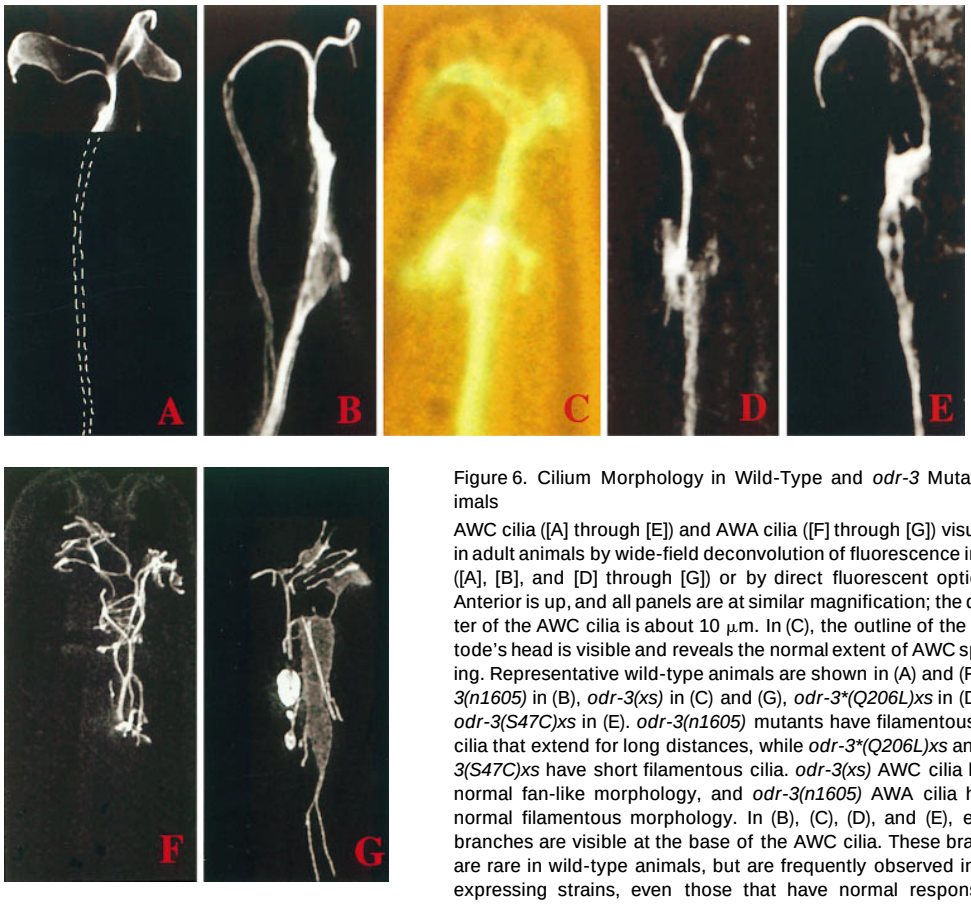

Figure 6. Cilium Morphology in Wild-Type and *odr-3* Mutant Animals

AWC cilia ([A] through [E]) and AWA cilia ([F] through [G]) visualized in adult animals by wide-field deconvolution of fluorescence images ([A], [B], and [D] through [G]) or by direct fluorescent optics (C). Anterior is up, and all panels are at similar magnification; the diameter of the AWC cilia is about 10 μm. In (C), the outline of the nematode's head is visible and reveals the normal extent of AWC spreading. Representative wild-type animals are shown in (A) and (F); *odr-3(n1605)* in (B), *odr-3(xs)* in (C) and (G), *odr-3*(Q206L)xs* in (D), and *odr-3(S47C)xs* in (E). *odr-3(n1605)* mutants have filamentous AWC cilia that extend for long distances, while *odr-3*(Q206L)xs* and *odr-3(S47C)xs* have short filamentous cilia. *odr-3(xs)* AWC cilia have a normal fan-like morphology, and *odr-3(n1605)* AWA cilia have a normal filamentous morphology. In (B), (C), (D), and (E), ectopic branches are visible at the base of the AWC cilia. These branches are rare in wild-type animals, but are frequently observed in GFP-expressing strains, even those that have normal responses to odorants.

monitored as a loss of their ability to take up the fluorescent dye DiO (Perkins et al., 1986). Wild-type, *odr-3(null)*, *odr-3(xs)*, *odr-3*(Q206L)xs*, and *odr-3(S47C)xs* animals all exhibited normal ASH dye filling, and their ASH cilia were normal when examined using an *sra-6::GFP* transgene (Troemel et al., 1995; data not shown). By contrast, animals with the activating Q205L mutation in a *gpa-3* transgene are defective in ASH dye filling (Zwaal et al., 1997).

Discussion

The ODR-3 Gα Protein Is Required for Olfaction, Osmosensation, and Mechanosensation

odr-3 is essential for normal responses to volatile odorants. Unlike the previously described *C. elegans* G proteins, which have either very widespread (G_o, G_q, G_s; Mendel et al., 1995; Segelat et al., 1995; Brundage et al., 1996; Korswagen et al., 1997) or very subtle (*gpa-2, gpa-3*; Zwaal et al., 1997) functions, ODR-3 is strongly and selectively implicated in olfactory function. Its expression in the AWA, AWB, and AWC olfactory neurons is consistent with previous evidence implicating G protein–coupled receptors in *C. elegans* olfaction. G protein–coupled receptors are also central to mammalian olfaction, but just as *C. elegans* olfactory receptors are distinct from the mammalian receptors, the *C. elegans* G protein ODR-3 is distinct from the G_s-like vertebrate G protein G_{olf}. These data, together with expression data from vomeronasal neurons and insect olfactory neurons, suggest that a variety of signaling pathways will operate in chemosensation.

Unexpectedly, we find that the ODR-3 Gα protein is also essential for osmosensation and mechanosensation. These effects are likely to be due to ODR-3 Gα action within the ASH sensory cilia. The ASH neurons may be analogous to the pain-sensing neurons of mammals that mediate avoidance of a wide array of noxious stimuli; our results with ODR-3 suggest that G protein–coupled receptors will initiate or regulate nociception.

One surprising aspect of *odr-3* function is that it acts in neurons that appear to use different sensory transduction pathways (Figure 7). *odr-3* is essential for all functions of the ASH and AWA neurons; the only other gene known to be required in these two neurons is *osm-9*, which encodes a novel predicted channel with extensive similarity to the capsaicin–sensitive receptor that is important in mammalian pain sensation (Caterina et al., 1997; Colbert et al., 1997). OSM-9 and the capsaicin receptor are more distantly related to the G protein–regulated *Drosophila* phototransduction channel TRP/TRPL (Tsunoda et al., 1997). Since ODR-3 and OSM-9

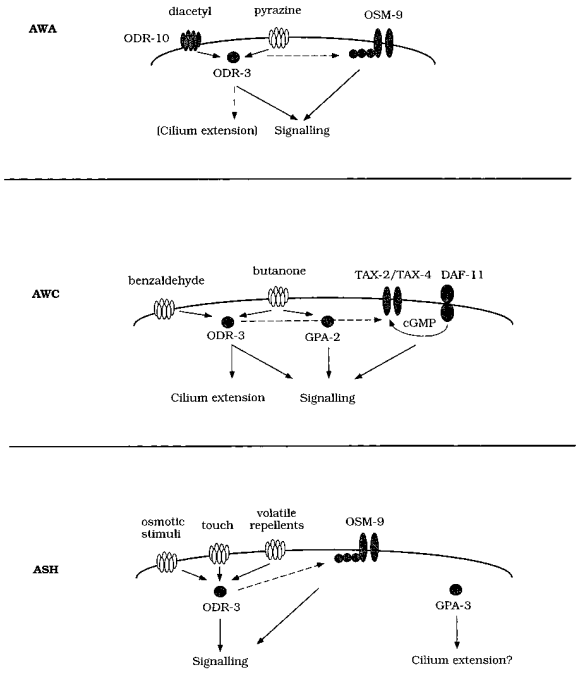

Figure 7. Summary of Gα Function in Different Chemosensory Neurons

Shaded molecules are cloned, whereas unshaded receptors are hypothetical. The putative channels TAX-2, TAX-4, and OSM-9 represent potential targets for ODR-3 function (dotted lines). *odr-3* is essential for signaling in AWA, AWC, and ASH; it affects cilium morphology in AWC and can affect AWA cilium morphology when overexpressed.

functions are so similar in AWA and ASH, we speculate that the OSM-9/capsaicin receptor channel family will be regulated by G proteins such as ODR-3 and G_i.

By contrast, the olfactory function of the AWC olfactory neurons requires *odr-3,* a cyclic nucleotide–gated channel encoded by *tax-2* and *tax-4,* and a transmembrane guanylyl cyclase encoded by *daf-11* (Coburn and Bargmann, 1996; Komatsu et al., 1996; D. Birnby and J. H. Thomas, personal communication), suggesting that *odr-3* regulates cyclic nucleotide production or degradation. *odr-3* could be a bifunctional G protein that couples to two signaling systems; alternatively, some of these neurons could require both *odr-3* and another G protein whose function has not been tested (e.g., *C. elegans* G_o, G_q, and G_s are all widely expressed, but these mutants move too poorly to be tested for sensory function).

odr-3 Activity Specifies the Shape of Olfactory Cilia

The reciprocal effects of *odr-3* levels on AWA and AWC cilia indicate that the amount of ODR-3 protein can determine the extent of cilium outgrowth. Like olfactory neurons in other animals, the AWA and AWC neurons have cilia with modified structures that may allow efficient odorant capture (Figures 1A and 1B). The AWA cilia are split into a large array of slender filamentous branches, whereas the AWC cilia extend in two fan-like flat sheets. Since alteration of ODR-3 levels can cause reciprocal transformations between AWA and AWC morphologies, we propose that ODR-3 expression defines the unique fan-like extension of the AWC olfactory cilia.

Complex differentiated cilia and associated structures are characteristic of many types of sensory neurons. The *odr-3* phenotypes implicate heterotrimeric G protein signaling in cilium morphogenesis. There are two general ways in which *odr-3* could act: it could interact with a specific ligand–activated receptor that controls cilium development, or it could be part of a homeostatic mechanism that allows odorant–induced signaling to regulate the shape of the sensory cilia. Although there is no previous evidence for G protein function in cilium development, G proteins in other systems can contribute to cell polarity and morphogenesis. G protein–coupled receptors direct chemotaxis of leukocytes and *Dictyostelium* amoebae by reorganizing the actin cytoskeleton (Klotz and Jesaitis, 1994; Parent and Devreotes, 1996), and a *C. elegans* Gβ subunit is required to orient the polarity of embryonic cell divisions (Zwaal et al., 1996).

In *C. elegans*, at least 25 genes are required for normal structure of the sensory cilia, which are the only cilia in the animal (Starich et al., 1995). Nineteen candidate Gα proteins are encoded in the sequenced regions of the *C. elegans* genome, including a G_s, a G_o, a G_q, and at least 10 Gα proteins of unknown function (Mendel et al., 1995; Segalat et al., 1995; Brundage et al., 1996; Korswagen et al., 1997; G. Jansen and R. Plasterk, personal communication). Perhaps some of the other G proteins also determine specific cilium properties. It is interesting that *gpa-3*(Q205L)* mutations, unlike *odr-3* (Q206L)* mutations, affect the ability of the ASH cilia to take up the fluorescent dye DiO (Zwaal et al., 1997).

Mutations that affect signal transduction components can indirectly cause cilium degeneration (Ranganathan et al., 1995). *Drosophila*, mouse, and human mutations that affect phototransduction cause degeneration, but not proliferation, of the photosensitive structures (Chang et al., 1993; Ranganathan et al., 1995; Sullivan and Daiger, 1996). *odr-3* is unlike these genes, since alteration of *odr-3* can either decrease or increase the area of olfactory cilia. However, the severe AWC alterations observed in *odr-3*(Q206L)xs* and *odr-3(S47C)xs* strains might represent degenerative events caused by aberrant signaling.

Are all of the behavioral effects of *odr-3* due to its effects on cilia? Probably not: although malformation of the cilia probably decreases odorant sensitivity to some degree, the visible cilium defects cannot account for all *odr-3* sensory defects. For example, the *odr-3(xs)* strain has appropriately extended AWC cilia and major defects in AWC-mediated olfaction, whereas the *odr-3(S47C)* strain has very severe AWC cilium defects and milder AWC olfactory defects. Moreover, the AWC neurons of *odr-3* null mutants have severe defects in cilium morphology, but the AWA neurons are at most mildly affected, and the ASH neurons appear morphologically normal. Yet, *odr-3* null mutants are more defective in AWA and ASH behaviors than they are in AWC behaviors (Bargmann et al., 1993). The AWA cilia of *che-2* mutants are far more distorted than those of *odr-3* mutants (Lewis and Hodgkin, 1977), but *che-2* mutants are only

mildly defective in chemotaxis to diacetyl, whereas *odr-3* mutants are severely defective (Bargmann et al., 1993). This result suggests that ODR-3 is directly involved in diacetyl detection, perhaps through interaction with the diacetyl receptor ODR-10.

Chemosensory Gα Proteins Have Distinct but Partly Overlapping Functions

Unlike vertebrate olfactory neurons, individual *C. elegans* olfactory neurons express several odorant receptors and integrate information about multiple odorants (Bargmann et al., 1993; Troemel et al., 1995; Sengupta et al., 1996); our studies with *odr-3* indicate that individual sensory neurons can also utilize more than one Gα protein. The AWC neurons detect both benzaldehyde and butanone, and *odr-3* mutants are severely defective in benzaldehyde chemotaxis but only mildly defective for butanone chemotaxis, whereas animals doubly mutant for *odr-3* and the similar protein *gpa-2* are severely defective in butanone chemotaxis. *gpa-2* and *gpa-3* have been previously implicated in developmental responses to the *C. elegans* dauer pheromone (Zwaal et al., 1997).

Despite the sequence similarity between *odr-3* and the *gpa* proteins, *gpa-2* is unable to substitute for most functions of *odr-3* in the AWC neurons where both are expressed, and *gpa-3* cannot substitute for *odr-3* in the avoidance function of the ASH neurons. Conversely, activated *gpa-3*(Q205L)* mutations affect the ability of the ASH neurons to take up the dye DiO but do not cause ASH sensory defects (Zwaal et al., 1997), whereas *odr-3*(Q206L)* mutations affect ASH sensory function but not ASH dye filling. This difference between *odr-3* and *gpa-3* implies that they interact with different effectors in ASH; one intriguing possibility is that *gpa-3* has a role in ASH cilium morphology that is analogous to the role of *odr-3* in AWC cilium morphology.

Responses to high concentrations of some odorants persist in *odr-3* null mutants (Bargmann et al., 1993) and even in *gpa-2 odr-3* double mutants (data not shown). Likewise, a residual olfactory response persists in G_{olf} knockout mice (Belluscio et al., 1998 [this issue of *Neuron*]). Similar observations were made in studies of the effects of gustducin mutations on mouse taste: gustducin-deficient mice have a 10- to 100-fold decrease in their sensitivity to sweet or bitter taste, depending on the assay, but they respond well to high concentrations of tastants (Wong et al., 1996). The residual response in gustducin mutants might be due to transducin, which is expressed in taste buds at lower levels (Ruiz-Avila et al., 1995). Unlike photoreceptors, which link rhodopsin to a single Gα protein, chemosensory neurons may be able to deploy families of Gα proteins during transduction. This distinction may arise from the fundamental differences between visual and olfactory reception. In the visual system, a few closely related opsin genes are responsible for all responses to light. By contrast, different chemosensory neurons contain widely divergent receptor proteins. There are at least three independent families comprising hundreds of vertebrate chemosensory receptor genes (Buck and Axel, 1991; Dulac and Axel, 1995; Herrada and Dulac, 1997; Matsunami and Buck, 1997; Ryba and Tirindelli, 1997) and at least four independent families comprising hundreds of *C. elegans* chemosensory receptor genes (Troemel et al., 1995; Sengupta et al., 1996). G protein diversity may follow naturally from the receptor diversity involved in chemoreception.

Experimental Procedures

Strains

Wild-type animals were *C. elegans* variety Bristol, strain N2. Nematodes were grown at 20°C with plentiful food using standard methods (Brenner, 1974).

Strains used in this work included MT3644 *odr-3(n1605)* V, CX2818 *lin-15(n765ts)* X, CX2695 *odr-3(n2150)* V *lin-15(n765)* X, GS357 *unc-42(e270) arDf1* V/*nT1 (n754)* IV, BW163 *ctDf1* V/*nT1 (n754)* IV, MT5817 *nDf42* V/*nT1 (n754)* IV, CX2369 *dpy-11(e224) odr-3(n2150)* V, GS352 *rol-4(sc63) arP3 arP1 unc-76(e911)* V, NL334 *gpa-2(pk16)* V, and DA869 *rol-4(sc8) lin-25(n545) him-5(e1467) unc-76(e911)* V.

Genetic Mapping and Cloning of *odr-3*

odr-3 had previously been mapped to the interval between *sqt-3* and *unc-61* on linkage group V (Bargmann et al., 1993). Subsequent mapping experiments localized the *odr-3* gene between the polymorphism *arP3* and the gene *eat-6,* as summarized below. The genetic deficiency *arDf1* complemented the *odr-3(n2150)* defects in osmotic avoidance and chemotaxis to benzaldehyde, indicating that it does not delete the *odr-3* gene. Since the *eat-6* locus is uncovered by *arDf1*, *odr-3* is to the right of *eat-6*. *arP3* is a Tc1-associated polymorphism, which is not deleted by *arDf1* (Tuck and Greenwald, 1995). *odr-3(n2150)* animals were mated with *rol-4(sc63) arP3 arP1 unc-76(e911)* V hermaphrodites. Nine out of 35 Rol non-Unc recombinants had lost the *arP3* polymorphism, and seven out of nine of these recombinants segregated *odr-3(n2150)*. This analysis placed *odr-3* to the left of *arP3*.

Overlapping cosmids from this region of the genome were introduced into *odr-3(n2150)* animals, and the resulting transgenic strains were tested for the ability to avoid areas of high osmotic strength (4 M fructose). Two overlapping cosmids, C34D1 and C34A12, were able to rescue the osmotic-avoidance defect of *odr-3(2150)* mutants. Subclones from the region shared by both cosmids were injected to define the region containing the rescuing activity. A 7 kb EcoRV subclone (pODR3-1) rescued the osmotic-avoidance phenotype and was also sufficient to rescue the ability of *odr-3(n2150)* animals to respond to all odorants and to avoid octanol.

A 9 kb EcoRI-SphI fragment from the rescuing region was used to screen $\sim 1 \times 10^6$ plaques of a mixed stage *C. elegans* cDNA library. Three positive clones were isolated (Figure 2). Two cDNAs encoded proteins that were fully contained in a subclone that failed to rescue the *odr-3* mutant phenotype. The remaining clone encoded a partial cDNA with a high degree of homology to α subunits of heterotrimeric G proteins (Gα). Reverse transcription-PCR experiments with *C. elegans* splice leader sequences SL1 and SL2 indicated that the Gα message was trans-spliced to SL1 at its extreme 5′ end, so the SL1 splice leader was used as a 5′ primer in RT-PCR reactions to isolate a full-length cDNA clone from mixed-stage wild-type animals. The coding sequence of the Gα was fully contained in the rescuing EcoRV subclone and was partially or entirely deleted from all subclones that failed to rescue, indicating that the Gα coding region corresponded to the *odr-3* gene.

Behavioral Assays

Chemotaxis assays were performed on a round assay plate with a point source of attractant at one end and a control spot of diluent at the opposite end (Bargmann et al., 1993). The chemotaxis index was calculated as [(animals at attracant) − (animals in control area)]/(total number of animals).

Osmotic avoidance assays were performed as described (Culotti and Russell, 1978). Animals were placed within a high osmotic strength ring of 4 M fructose and counted after 10 min. The osmotic avoidance index was calculated as the fraction of worms still in the ring at the end of the assay.

Volatile avoidance assays and nose-touch assays were performed as described (Kaplan and Horvitz, 1993; Troemel et al., 1995).

Germline Transformation

Germline transformations were performed using standard microinjection methods (Mello et al., 1991). All transformations were performed in strains containing *lin-15(n765)* with or without *odr-3* mutations. Coinjection mixes consisted of *lin-15* DNA pJM23 (50 ng/μl) and experimental DNA at various concentrations (5–100 ng/ml). Transgenic animals were identified by rescue of the multivulva phenotype of *lin-15(n765)* animals at 20°C. Independent lines were established from single rescued F1 animals. Transgenes were integrated using γ rays (Mello et al., 1991) or trimethylpsoralen treatment followed by UV irradiation (A. Santoso and C. I. B., unpublished data).

Molecular Biology Methods

General manipulations were performed using standard protocols (Sambrook et al., 1989). Genomic DNA from the mutant alleles was amplified by PCR, and purified PCR products were sequenced directly. Sequencing was performed with the *fmol* sequencing kit (Promega) and an MJR thermal cycler. The Geneworks software package (Intelligenetics) was used in sequence analysis. BLAST (Altschul et al., 1990), CLUSTAL W (Thompson et al., 1994), and PHYLIP (Felsenstein, 1996) packages were used to perform sequence comparisons and construct phylogenetic trees. Sequence of the *odr-3* region was confirmed with data courtesy of the *C. elegans* genome sequencing consortium, who identified this region as predicted gene C34D1.3 (Sulston et al., 1992). PCR reactions were performed using the following buffer: 50 mM KCl, 1.5 mM $MgCl_2$, 10 mM Tris-HCl (pH 8.3), and 0.01% gelatin. Primers used in sequencing and PCR are available upon request.

Antibody Staining

Antigen Preparation

A GST fusion was made to the last 106 amino acids of the *odr-3* coding region and injected into rabbits. Polyclonal sera were affinity-purified by binding to 6HIS-tagged full-length ODR-3 protein coupled to Affigel-15 resin (Biorad) and eluted with 3.5 M $MgCl_2$.

Staining

Animals were spread onto 0.1% polylysine-coated slides, heated on a 100°C block for 20 s, frozen on dry ice, and fixed by incubation in methanol (−20°C) for 5 min followed by incubation in acetone (−20°C) for 5 min. Samples were blocked in blocking solution (1× phosphate-buffered saline (PBS), 1% BSA (Sigma), 0.1% Tween-20) for 1 hr at room temperature, incubated with a 1:50 dilution of affinity-purified antibody overnight at 4°C, washed with PBS, incubated with a 1:500 dilution of Cy3 goat anti-rabbit IgG (Jackson Immunochemicals) at room temperature for 1 hr, and washed with PBS. DAPI (1 μg/ml) was included to stain nucleic acids in the samples. All larval stages and adults showed comparable staining.

Generation and Analysis of *odr-3* Expression Constructs

pODR3::GFP-1

A 2.7 kb HindIII fragment of pRV-1 was excised and ligated into the HindIII site of pTU#62 (Chalfie et al., 1994).

pODR-3::GFP-2

A fragment from the EcoRV site to the ATG of *odr-3* was amplified from pODR3-1 and ligated into the SmaI site of pPD95.77 (A. Fire, S. Xu, N. Ahnn, and G. Seydoux, personal communication).

All cells expressing the pODR-3::GFP-2 promoter fusion were identified in two independent integrated lines bearing the transgene. AWC had the strongest and most reliable expression (25 of 25 animals were GFP-positive), followed by AWB (22 of 25), AWA (8 of 25), ADF (6 of 25), and ASH (5 of 25). The GFP expression was always brightest in AWC, less bright in AWB, and faint in the other three cells, suggesting that AWA, ADF, and ASH express GFP at near the detection threshold. All larval stages and adults showed comparable expression. To ask whether other sequences in the *odr-3* introns or upstream region affect expression, we stained animals that overexpressed the 7 kb rescuing *odr-3* genomic clone with an anti-ODR-3 antibody. In the overexpressing lines, ODR-3 protein was in the cell bodies as well as the cilia, providing more information than was available with the highly localized endogenous ODR-3 protein. All animals showed a cluster of five cells consistent with the cells named above (rigorous cell identification was not always possible in fixed animals). The five sensory neurons had approximately equal staining intensities. Some animals also showed weak staining of another cell, probably the interneuron AIN.

Generation and Analysis of *odr-3* Mutants

The *odr-3(S47C)* and the *odr-3(Q206L)* mutants were generated in *odr-3* subclones using specific PCR primers to create the mutations, sequenced, and reintroduced into the genomic pODR3-1 clone. Clones were injected into *odr-3(+)* animals at either 10 ng/ml or 100 ng/ml, and into *odr-3(n1605)* animals at 10 ng/ml, using the *lin-15* cotransformation marker.

Microscopy

Images in Figure 6 were acquired with a scientific grade cooled CCD camera on a multiwavelength wide-field three-dimensional microscopy system (Hiraoka et al., 1991) in which the shutters, filters, and XYZ stage are all computer-driven. Samples were imaged using a 60× 1.4 NA lens (Olympus) and n = 1.1518 immersion oil. Three-dimensional data stacks of GFP-expressing samples were acquired in the FITC channel by moving the stage in successive 0.25 μm focal planes through the sample, and out-of-focus light was removed with a constrained iterative deconvolution algorithm (Agard et al., 1989). Maximum intensity projections of the three-dimensional data stacks were generated using IVE software (Chen et al., 1996).

Other images were acquired by conventional fluorescence microscopy using a Zeiss Axioplan II microscope and a 40× Plan Apochromat objective.

Acknowledgments

We are grateful to Orion Weiner and John Sedat for their guidance in deconvolution microscopy. We thank Henry Bourne, Ira Herskowitz, Richard Axel, Sue Kirch, Jen Zallen, and Emily Troemel for discussion and comments on the manuscript; Hernan Espinoza, Andrew Shiau, and Ramon Tabtiang for advice, reagents, and valuable discussions; Jim Thomas for the *odr-3(n1605)* strain; Simon Tuck and Iva Greenwald for the *arP3* strain; Bob Barstead for the cDNA library; Emily Troemel for the STR-2::GFP fusion gene; Andy Fire for the GFP vector; and the *Caenorhabditis* Genetic Center for some strains used in this work. This work was supported by the Howard Hughes Medical Institute. K. R., J. G. C., and A. S. are Predoctoral Fellows of the Howard Hughes Medical Institute, and C. I. B. is an Assistant Investigator of the Howard Hughes Medical Institute.

Received October 28, 1997; revised December 2, 1997.

References

Agard, D.A., Hiraoka, Y., Shaw, P., and Sedat, J.W. (1989). Fluorescence microscopy in three dimensions. Methods Cell Biol. *30*, 353–377.

Altschul, S.F., Gish, W., Miller, W., Myers, E.W., and Lipman, D.J. (1990). Basic local alignment search tool. J. Mol. Biol. *215*, 403–410.

Barber, V.C. (1974). Cilia in sense organs. In Cilia and Flagella, M.A. Sleigh, ed. (London: Academic Press), pp. 403–433.

Bargmann, C.I., and Mori, I. (1997). Chemotaxis and thermotaxis. In *C. elegans* II, T.B.D.L. Riddle, B.J. Meyer, J.R. Priess, eds. (Cold Spring Harbor, NY: Cold Spring Harbor Laboratory Press), pp. 717–737.

Bargmann, C.I., Hartwieg, E., and Horvitz, H.R. (1993). Odorant-selective genes and neurons mediate olfaction in C. elegans. Cell *74*, 515–527.

Belluscio, L., Gold, G.H., Nemes, A., and Axel, R. (1998). Mice deficient in G_{olf} are anosmic. Neuron *20*, this issue, 69–81.

Berghard, A., and Buck, L.B. (1996). Sensory transduction in vomeronasal neurons: evidence for Gαo, Gαi2, and adenylyl cyclase II as major components of a pheromone signaling cascade. J. Neurosci. *16*, 909–918.

Brenner, S. (1974). The genetics of Caenorhabditis elegans. Genetics *77*, 71–94.

Brundage, L., Avery, L., Katz, A., Kim, U.-J., Mendel, J., Sternberg, P., and Simon, M. (1996). Mutations in a C. elegans $G_q\alpha$ gene disrupt movement, egg laying, and viability. Neuron *16*, 999–1009.

Buck, L., and Axel, R. (1991). A novel multigene family may encode odorant receptors: a molecular basis for odor recognition. Cell *65*, 175–187.

Caterina, M.J., Schumacher, M.A., Tominaga, M., Rosen, T.A., Levine, J.D., and Julius, D. (1997). The capsaicin receptor: a heat-activated ion channel in the pain pathway. Nature *389*, 816–824.

Chalfie, M., Tu, Y., Euskirchen, G., Ward, W.W., and Prasher, D.C. (1994). Green fluorescent protein as a marker for gene expression. Science *263*, 802–805.

Chang, G.Q., Hao, Y., and Wong, F. (1993). Apoptosis: final common pathway of photoreceptor death in rd, rds, and rhodopsin mutant mice. Neuron *11*, 595–605.

Chen, H., Hughes, D.D., Chan, T.A., Sedat, J.W., and Agard, D.A. (1996). IVE (Image Visualization Environment): a software platform for all three-dimensional microscopy applications. J. Struct. Biol. *116*, 56–60.

Coburn, C.M., and Bargmann, C.I. (1996). A putative cyclic nucleotide–gated channel is required for sensory development and function in C. elegans. Neuron *17*, 695–706.

Colbert, H.A., Smith, T.L., and Bargmann, C.I. (1997). OSM-9, a novel protein with structural similarity to channels, is required for olfaction, mechanosensation, and olfactory adaptation in C. elegans. J. Neurosci. *17,* 8259–8269.

Conklin, B.R., and Bourne, H.R. (1993). Structural elements of $G\alpha$ subunits that interact with $G\beta\gamma$, receptors, and effectors. Cell *73*, 631–641.

Culotti, J.G., and Russell, R.L. (1978). Osmotic avoidance defective mutants of the nematode Caenorhabditis elegans. Genetics *90*, 243–256.

Dulac, C., and Axel, R. (1995). A novel family of genes encoding putative pheromone receptors in mammals. Cell *83*, 195–206.

Felsenstein, J. (1996). Inferring phylogenies from protein sequences by parsimony, distance, and likelihood methods. Methods Enzymol. *266*, 418–427.

Firestein, S., Zufall, F., and Shepherd, G.M. (1991). Single odor-sensitive channels in olfactory receptor neurons are also gated by cyclic nucleotides. J. Neurosci. *11*, 3565–3572.

Halpern, M., Shapiro, L.S., and Jia, C. (1995). Differential localization of G proteins in the opossum vomeronasal system. Brain Res. *677*, 157–161.

Herrada, G., and Dulac, C. (1997). A novel family of putative pheromone receptors in mammals with a topographically organized and sexually dimorphic distribution. Cell *90*, 763–773.

Hiraoka, Y., Swedlow, J.R., Paddy, M.R., Agard, D.A., and Sedat, J.W. (1991). Three-dimensional multiple-wavelength fluorescence microscopy for the structural analysis of biological phenomena. Semin. Cell Biol. *2*, 153–165.

Jones, D.T., and Reed, R.R. (1989). G_{olf}: an olfactory neuron specific-G protein involved in odorant signal transduction. Science *244*, 790–795.

Kaplan, J., and Horvitz, H. (1993). A dual mechanosensory and chemosensory neuron in *Caenorhabditis elegans*. Proc. Natl. Acad. Sci. USA *90*, 2227–2231.

Klotz, K.N., and Jesaitis, A.J. (1994). Neutrophil chemoattractant receptors and the membrane skeleton. Bioessays *16*, 193–198.

Komatsu, H., Mori, I., Rhee, J.-S., Akaike, N., and Ohshima, Y. (1996). Mutations in a cyclic nucleotide–gated channel lead to abnormal thermosensation and chemosensation in C. elegans. Neuron *17*, 707–718.

Korswagen, H.C., Park, J.H., Ohshima, Y., and Plasterk, R.H. (1997). An activating mutation in a Caenorhabditis elegans G_s protein induces neural degeneration. Genes Dev. *11*, 1493–1503.

Lewis, J.A., and Hodgkin, J.A. (1977). Specific neuroanatomical changes in chemosensory mutants of the nematode Caenorhabditis elegans. J. Comp. Neurol. *172*, 489–510.

Lochrie, M.A., Mendel, J.E., Sternberg, P.W., and Simon, M.I. (1991). Homologous and unique G protein α subunits in the nematode *Caenorhabditis elegans*. Cell Reg. *2*, 135–154.

Matsunami, H., and Buck, L.B. (1997). A multigene family encoding a diverse array of putative pheromone receptors in mammals. Cell *90,* 775–784

Mello, C.C., Kramer, J.M., Stinchcomb, D., and Ambros, V. (1991). Efficient gene transfer in C. elegans: extrachromosomal maintenance and integration of transforming sequences. EMBO J. *10*, 3959–3970.

Mendel, J., Korswagen, H., Liu, K., Hadju-Cronin, Y., Simon, M., Plasterk, R., and Sternberg, P. (1995). Participation of the protein G_o in multiple aspects of behavior in *C. elegans*. Science *267*, 1652–1655.

Pace, U., Hanski, E., Salomon, Y., and Lancet, D. (1985). Odorant-sensitive adenylate cyclase may mediate olfactory reception. Nature *316*, 255–258.

Parent, C.A., and Devreotes, P.N. (1996). Molecular genetics of signal transduction in Dictyostelium. Annu. Rev. Biochem. *65*, 411–440.

Perkins, L.A., Hedgecock, E.M., Thomson, J.N., and Culotti, J.G. (1986). Mutant sensory cilia in the nematode Caenorhabditis elegans. Dev. Biol. *117*, 456–487.

Ranganathan, R., Malicki, D.M., and Zuker, C.S. (1995). Signal transduction in Drosophila photoreceptors. Annu. Rev. Neurosci. *18*, 283–317.

Rens-Domiano, S., and Hamm, H.E. (1995). Structural and functional relationships of heterotrimeric G-proteins. FASEB J. *9*, 1059–1066.

Ruiz-Avila, L., McLaughlin, S.K., Wildman, D., McKinnon, P.J., Robichon, A., Spickofsky, N., and Margolskee, R.F. (1995). Coupling of bitter receptor to phosphodiesterase through transducin in taste receptor cells. Nature *376*, 80–85.

Ryba, N.J.P., and Tirindelli, R. (1997). A new multigene family of putative pheromone receptors. Neuron *19,* 371–379.

Sambrook, J., Fritsch, E.F., and Maniatis, T. (1989). Molecular Cloning: A Laboratory Manual. (Cold Spring Harbor, NY: Cold Spring Harbor Press).

Segalat, L., Elkes, D., and Kaplan, J. (1995). G_o modulation of serotonin-controlled behaviors in *C. elegans*. Science *267*, 1648–1651.

Sengupta, P., Chou, J.C., and Bargmann, C.I. (1996). *odr-10* encodes a seven transmembrane domain olfactory receptor required for responses to the odorant diacetyl. Cell *84*, 899–909.

Slepak, V.Z., Quick, M.W., Aragay, A.M., Davidson, N., Lester, H.A., and Simon, M.I. (1993). Random mutagenesis of G protein α subunit $G(o)\alpha$. Mutations altering nucleotide binding. J. Biol. Chem. *268*, 21889–21894.

Slepak, V.Z., Katz, A., and Simon, M.I. (1995). Functional analysis of a dominant negative mutant of $G\alpha i2$. J. Biol. Chem. *270*, 4037–4041.

Starich, T.A., Herman, R.K., Kari, C.K., Yeh, W.H., Schackwitz, W.S., Schuyler, M.W., Collet, J., Thomas, J.H., and Riddle, D.L. (1995). Mutations affecting the chemosensory neurons of Caenorhabditis elegans. Genetics *139*, 171–188.

Sullivan, L.S., and Daiger, S.P. (1996). Inherited retinal degeneration: exceptional genetic and clinical heterogeneity. Molec. Med. Today *2*, 380–386.

Sulston, J., Du, Z., Thomas, K., Wilson, R., Hillier, L., Staden, R., Halloran, N., Green, P., Thierry-Mieg, J., Qiu, L., et al. (1992). The C. elegans genome sequencing project: a beginning. Nature *356*, 37–41.

Talluri, S., Bhatt, A., and Smith, D.P. (1995). Identification of a Drosophila G protein alpha subunit (dGq alpha-3) expressed in chemosensory cells and central neurons. Proc. Natl. Acad. Sci. USA *92*, 11475–11479.

Tamar, H. (1992). Principles of Sensory Physiology (Springfield, IL: Charles C. Thomas).

Thompson, J.D., Higgins, D.G., and Gibson, T.J. (1994). CLUSTAL W: improving the sensitivity of progressive multiple sequence alignment through sequence weighting, position-specific gap penalties and weight matrix choice. Nucleic Acids Res. *22*, 4673–4680.

Troemel, E.R., Chou, J.H., Dwyer, N.D., Colbert, H.A., and Bargmann,

C.I. (1995). Divergent seven transmembrane receptors are candidate chemosensory receptors in C. elegans. Cell *83*, 207–218.

Troemel, E.R., Kimmel, B.E., and Bargmann, C.I. (1997). Reprogramming chemotaxis responses: sensory neurons define olfactory preferences in C. elegans. Cell *91*, 161–169.

Tsunoda, S., Sierralta, J., Sun, Y., Bodner, R., Suzuki, E., Becker, A., Socolich, M., and Zuker, C.S. (1997). A multivalent PDZ-domain protein assembles signaling complexes in a G-protein-coupled cascade. Nature *388*, 243–249.

Tuck, S., and Greenwald, I. (1995). *lin-25,* a gene required for vulval induction in Caenorhabditis elegans. Genes Dev. *9*, 341–357.

Ward, S., Thomson, N., White, J.G., and Brenner, S. (1975). Electron microscopical reconstruction of the anterior sensory anatomy of the nematode Caenorhabditis elegans. J. Comp. Neurol. *160*, 313–337.

Ware, R.W., Clark, D., Crossland, K., and Russell, R.L. (1975). The nerve ring of the nematode *Caenorhabditis elegans*: sensory input and motor output. J. Comp. Neurol. *162*, 71–110.

Wedegaertner, P.B., Wilson, P.T., and Bourne, H.R. (1995). Lipid modifications of trimeric G proteins. J. Biol. Chem. *270*, 503–506.

Wong, G.T., Gannon, K.S., and Margolskee, R.F. (1996). Transduction of bitter and sweet taste by gustducin. Nature *381*, 796–800.

Woodard, C., Alcorta, E., and Carlson, J. (1992). The *rdgB* gene of *Drosophila:* a link between vision and olfaction. J. Neurogenet. *8*, 17–31.

Zhang, Y., Chou, J.H., Bradley, J., Bargmann, C.I., and Zinn, K. (1997). The *C. elegans* 7-transmembrane protein ODR-10 functions as an odorant receptor in mammalian cells. Proc. Natl. Acad. Sci. USA *94*, 12162–12167.

Zwaal, R., Ahringer, J., van Leunen, H., Rushforth, A., Anderson, P., and Plasterk, R. (1996). G proteins are required for spatial orientation of early cell cleavages in C. elegans embryos. Cell *84*, 619–629.

Zwaal, R.R., Mendel, J.E., Sternberg, P.W., and Plasterk, R.H.A. (1997). Two neuronal G proteins are involved in chemosensation of the Caenorhabditis elegans dauer-inducing pheromone. Genetics *145*, 715–727.